Role of the COOH-terminal Nonhelical Tailpiece in the Assembly of a Vertebrate Nonmuscle Myosin Rod

Tony P. Hodge, Robert Cross, and John Kendrick-Jones

MRC Laboratory of Molecular Biology, Hills Road, Cambridge, CB2 2QH, United Kingdom

Abstract. A short nonhelical sequence at the COOH-terminus of vertebrate nonmuscle myosin has been shown to enhance myosin filament assembly. We have analyzed the role of this sequence in chicken intestinal epithelial brush border myosin, using protein engineering/site-directed mutagenesis. Clones encoding the rod region of this myosin were isolated and sequenced. They were truncated at various restriction sites and expressed in *Escherichia coli*, yielding a series of mutant myosin rods with or without the COOH-terminal tailpiece and with serial deletions from their NH_2-termini. Deletion of the 35 residue COOH-terminal nonhelical tailpiece was sufficient to increase the critical concentration for myosin rod assembly by 50-fold (at 150 mM NaCl, pH 7.5), whereas NH_2-terminal deletions had only minor effects. The only exception was the longest NH_2-terminal deletion, which reduced the rod to 119 amino acids and rendered it assembly incompetent. The COOH-terminal tailpiece could be reduced by 15 amino acids and it still efficiently promoted assembly. We also found that the tailpiece promoted assembly of both filaments and segments; assemblies which have different molecular overlaps. Rod fragments carrying the COOH-terminal tailpiece did not promote the assembly of COOH-terminally deleted material when the two were mixed together. The tailpiece sequence thus has profound effects on assembly, yet it is apparently unstructured and can be bisected without affecting its function. Taken together these observations suggest that the nonhelical tailpiece may act sterically to block an otherwise dominant but unproductive molecular interaction in the self assembly process and does not, as has been previously thought, bind to a specific target site(s) on a neighboring molecule.

MYOSIN II (hereafter referred to as myosin) is a major constituent of eukaryotic contractile systems (Warwick and Spudich, 1987). It is present in sarcomeric and smooth muscles and also in nonmuscle tissues (cytoplasmic myosins). Structurally, the myosin molecule is a hexamer composed of two heavy chains (MHC),[1] two essential light chains and two regulatory light chains. The heavy chains are organized into two globular head regions where the force generating actin-binding and ATPase functions are located and a tail region composed of an α-helical coiled coil rod involved in filament assembly (Harrington and Rogers, 1984).

Myosins are monomeric in high ionic strength solutions (>300 mM NaCl) but assemble into filaments at low ionic strength. Such filament assembly behavior is believed to occur as a multistep process probably involving different regions of the myosin tail (Sinard et al., 1989). First an initial interaction between two or more myosin molecules occurs (nucleation) to form small bipolar assemblies (Reisler et al., 1980; Sinard and Pollard, 1989) followed by the parallel addition of further molecules to form a filament (elongation) (Davis, 1988; Sinard et al., 1989; Cross et al., 1991). Although most myosin filaments exhibit an axial 14.3-nm periodicity reflecting the packing of the myosin tails in the filament (Squire, 1981; McLachlan, 1984; Quinlan and Stewart, 1987) the purified myosins exhibit a range of assembly properties. For example, if one compares vertebrate smooth muscle and nonmuscle myosins with sarcomeric myosins there are differences in their critical concentrations for filament assembly (Josephs and Harrington, 1968; Megerman and Lowey, 1981; Kendrick-Jones et al., 1987), in their mode of nucleation/filament assembly (Cross et al., 1991) and in the structure and stability of their filaments (Craig and Megerman, 1977; Hinssen et al. 1978; Suzuki et al., 1978). In addition, vertebrate smooth muscle and nonmuscle myosins can exist in a dynamic equilibrium between folded monomer and assembled filament states regulated by light chain phosphorylation (Suzuki et al., 1978; Trybus et al., 1982; Craig et al., 1983). In this paper we have sought to identify those regions of the myosin tail which may be responsible for these differences in assembly behavior.

Although there is general heterogeneity in the amino acid sequences of vertebrate sarcomeric, smooth, and nonmuscle myosin rods, closer analysis reveals the presence of a com-

Robert Cross's present address is Marie Curie Research Institute, The Chart, Oxted, Surrey RH8 0TL.

1. *Abbreviations used in this paper*: KCNS, potassium thiocyanate; LMM, light meromyosin; MHC, myosin heavy chain; PCR, polymerase chain reaction.

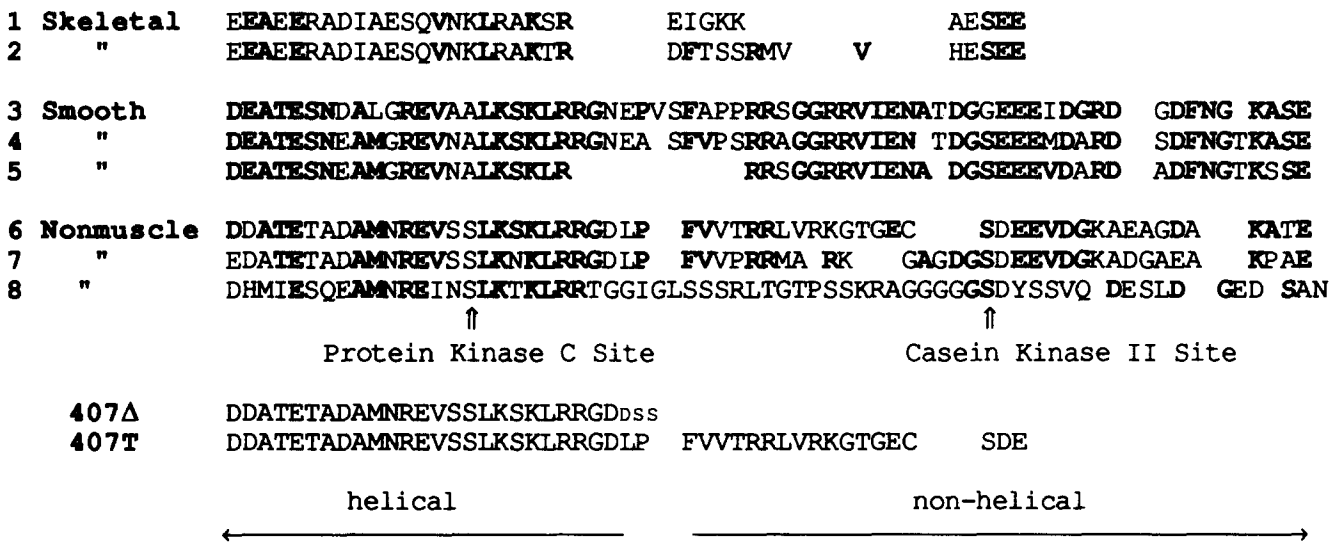

Figure 1. The COOH-terminal sequences of vertebrate sarcomeric, smooth and nonmuscle MHCs. (*1*) Chicken sarcomeric (*skeletal*) MHC (Molina et al., 1987); (*2*) rat embryo sarcomeric (*skeletal*) MHC (Strehler et al., 1986); (*3*) chicken smooth muscle MHC (Yanagisawa et al., 1987); (*4*) rat neonatal aorta MHC (Babij and Periasamy, 1989); (*5*) rabbit uterus MHC (Nagai et al., 1988); (*6*) chicken brush border MHC (this study); (*7*) human nonmuscle MHC (Saez et al., 1990); and (*8*) *Drosophila* nonmuscle MHC (Ketchum et al., 1990). Also shown are two of the expressed fragments; *407Δ*, nonmuscle rod fragment (407 amino acids) with deleted COOH terminus (last 35 amino acids deleted); and *407T*, the same rod fragment with the last 15 amino acids deleted. The sequences are grouped together according to tissue origin and aligned according to Dibb et al. (1989). Residues where an apparent consensus exists in smooth and/or nonmuscle myosins are in bold type and those residues reported to be phosphorylated are indicated (Kelley et al., 1991).

mon 28-amino acid repeating unit containing four heptad repeats, characteristic of coiled-coil molecules, with hydrophobic residues at the first and fourth positions within the heptad (Cohen and Parry, 1990). The most striking difference between these myosins is at their carboxyl termini where the smooth muscle and nonmuscle myosin rods contain a 35–43 residue nonhelical COOH-terminal tailpiece which is absent in sarcomeric myosin rods (Strehler et al., 1986; Molina et al., 1987; Yanagisawa et al., 1987; Nagai et al., 1988; Babij and Periasamy, 1989; Dibb et al., 1989; Shohet et al., 1989) (Fig. 1). The contrasting roles of sarcomeric myosins which form highly ordered, stable filament arrays in muscle and nonmuscle myosins which need to rapidly assemble and disassemble in cells for contractile events such as cytokinesis, has led to speculation that the nonmuscle myosin nonhelical tailpiece is the region responsible for directing the assembly and possibly the disassembly of this myosin. Removal of this COOH-terminal region from smooth muscle myosins by proteolytic cleavage (Cross and Vanderkerckhove, 1986; Ikebe et al., 1991) indicates that this region is required for self-assembly. The existence of phosphorylation sites within this tail piece in vertebrate nonmuscle myosins (Kelley et al., 1991) further strengthens the speculation that this domain may have a regulatory role in filament assembly/disassembly. Interestingly, alterations or modifications to the carboxyl termini of other myosins have also been shown to affect myosin filament assembly. For example, mutations in the COOH terminus of *Caenorhabditis elegans* unc-54 MHC disrupts myosin filament assembly (Dibb et al., 1985) while fusion proteins containing *Acanthamoeba* myosin II tail sequences with deletions in the last 100 amino acids fail to assemble (Sinard et al., 1990). However, phosphorylation or deletion of part of the nonhelical COOH-terminal tail piece of *Acanthamoeba* myosin II has little apparent effect on filament formation (Atkinson et al., 1989; Sathyamoorthy et al., 1990; Ganguly et al., 1990) whereas removal of the 17 COOH-terminal amino acids from rabbit skeletal muscle myosin rod disturbs filament assembly especially at high pH values (Maeda et al., 1991). Obviously the COOH-terminus is a crucial region for filament assembly in many types of myosins.

We have used a molecular biological approach to identify the specific regions of a vertebrate nonmuscle myosin rod involved in filament assembly and define the role of the nonhelical COOH-terminal tailpiece. We have isolated and sequenced clones encoding the myosin rod from a chicken intestinal epithelium (brush border cells) cDNA λ library, and have used these clones to construct recombinant protein expression plasmids designed to yield a series of truncated rod polypeptides for analysis in filament assembly experiments. By shortening the length of the expressed rod polypeptides progressively at the amino terminus in different constructs we have shown that a minimum length is required for assembly. Conversely, deletion of the COOH-terminal nonhelical tailpiece results in a dramatic increase in the critical concentration of rod polypeptide required for assembly which we believe results from an induced change in the association-dissociation kinetics of assembly. The data strongly suggest that the tailpiece favors assembly by inducing a favorable stagger between neighbors in the growing polymer. We discuss the possibility that productive staggers are forced by steric clashes between neighboring tailpieces.

Materials and Methods

Materials

Analytical grade reagents were used throughout and were obtained from

BDH Chemicals Ltd. (Poole, UK) and Bethesda Research Laboratories (Gaithersburg, MD). Radiochemicals were obtained from Amersham International (Amersham, UK). Papain, chymotrypsin, and hen egg white lysozyme were from Sigma Chemical Company (Poole, UK). All other enzymes were from New England Biolabs (Beverly, MA) or from Boehringer-Mannheim GmbH (Mannheim, Germany) and were used according to the manufacturer's standard assay conditions. Oligonucleotides were synthesized on an Applied Biosystems 380B automated DNA synthesizer (Applied Biosystems, Inc., Foster City, CA) by Jan Fogg and Terry Smith (MRC Laboratory of Molecular Biology, Cambridge, MA). The brush border λgt11 cDNA library was a generous gift from Dr. Paul Matsudaira (Whitehead Institute, Massachusetts Institute of Technology, Cambridge, MA). Chicken gizzards and intestines were obtained from G. W. Padley Ltd., (Bury St. Edmunds, UK).

Biochemical Methods

Chicken gizzard and brush border myosins and their light meromysin (LMM) and rod subfragments (for control experiments) were prepared as previously described (Kendrick-Jones et al., 1971, 1983; Citi and Kendrick-Jones, 1986). The protein concentrations of the myosin, native LMM, and rod fragments were estimated spectrophotometrically using the following absorption coefficients (A_{280} nm in 1-cm cells) for myosin 0.54, rod 0.30, and LMM 0.30 mg ml^{-1}. The concentrations of the expressed fragments were determined by the Pierce BCA protein assay (Pierce Chemical Co., Rockford, IL).

5–20% acrylamide gradient SDS-PAGE gels were run as described by Matsudaira and Burgess (1978) using the Pharmacia low molecular weight marker kit (14,000–94,000) for calibration (Pharmacia Chemicals, Piscataway, NJ). Glycerol-PAGE gels were used to analyze the purified rod fragments under nondissociating conditions. Gels (7.5% acrylamide 40% glycerol) were polymerized and electrophoresed in the following buffer: 0.122 M glycine, 0.02 M Tris, pH 8.6, and 40 mM sodium pyrophosphate, final pH ~8.9. For sample loading we included 10% 2-mercaptoethanol and 40% glycerol. Gels were run at 5 W constant power for 3 h. The proteins were visualised by staining with PAGE blue 83 (BDH Chemicals Ltd.). Western blots were carried out by the method of Burnette (1981) using brush border myosin mAbs BM1, BM3, and BM4 (Citi and Kendrick-Jones, 1987*b*) and were visualized using the Vector Laboratories ABC kit (Vector Laboratories Inc., Burlingame, CA).

DNA Manipulations

Unless otherwise stated, all DNA manipulations were performed as described in Sambrook et al. (1989). Bacteria harboring recombinant plasmids were grown in 2 × YT medium containing 50–100 μg ml^{-1} ampicillin. The chicken epithelial brush border λgt11 cDNA library was screened by the procedure described previously (Huynh et al., 1985) using brush border myosin mAbs BM1 and BM4 (Citi and Kendrick-Jones, 1987*b*), a biotinylated secondary antibody and an avidin-biotinylated HRP complex (Vector ABC kit, Vector Laboratories Inc.).

Initially 10 cDNA clones were identified after screening ~6 × 10^5 plaque forming units. Subcloning into pUC18 and restriction enzyme digestion analysis revealed that these were overlapping clones representing three cDNA clones derived from one transcript (Fig. 2). Restriction fragments from the 5′ end of our clones were used to reprobe the cDNA library, but unfortunately no new clones were detected. Similar results were observed by Shohet et al. (1989) using the same library but with different probes. We believe that during preparation of this cDNA library some artifact in the cDNA cloning process has blocked the reverse transcriptase from extending beyond the region represented in our clones.

Plasmid constructs, designed for bacterial expression of the desired polypeptides, were made in the relevant pINII vectors (Nakamura and Inouye, 1982), using the EcoRI or HindIII sites at the 5′ end and the BamHI at the 3′ end of the clones. (See Fig. 2 for details of clone manipulation.) Expression constructs with deleted nonhelical tailpieces were made either by deletion with restriction enzymes or by amplification from the original clone DNA by a polymerase chain reaction (PCR) method (Bunnell and Kidd, 1989). PCR products were digested with HindIII, a unique site in the original clones, and BamHI, introduced by the primer, and ligated into the expression clone.

Expression and Purification of Recombinant Proteins

The conditions for the bacterial expression of the rod constructs and the initial stages of purification were as described by Atkinson and Stewart (1991).

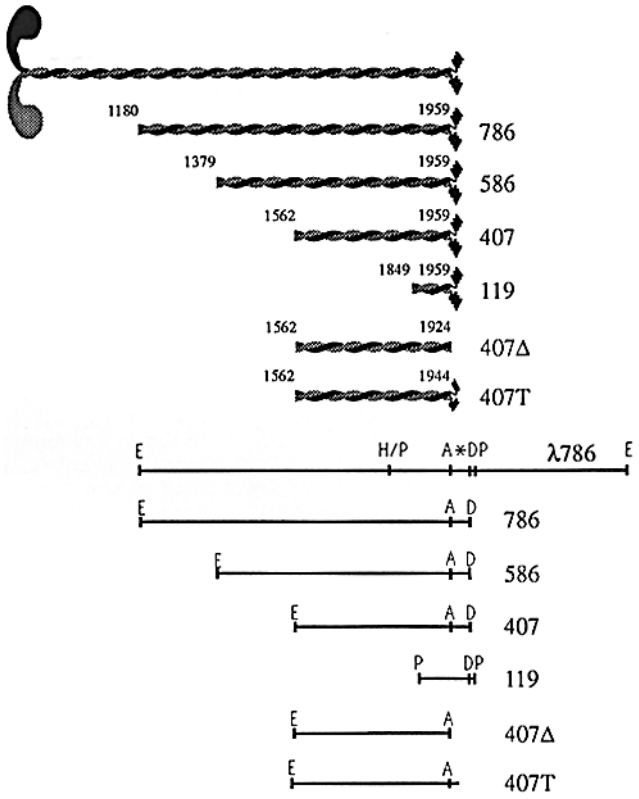

Figure 2. The expressed vertebrate nonmuscle myosin rod fragments. The expressed rod fragments are shown in diagrammatic form with α-helical coiled coils and nonhelical COOH termini. Also shown for comparison is intact myosin. They are labeled according to the number of amino acid residues present, including residues introduced by the cloning process. The first and last amino acid residues are numbered according to the published sequence (Shohet et al., 1989). Fragments *786*, *586*, *407*, and *119* have intact COOH termini; *407Δ* has no tailpiece and *407T* has a truncated tailpiece. The construct *407Δ* is an example of a set of COOH-terminal deletions made on all the intact fragments. A restriction map of the sites used for cloning the expression constructs is also shown beneath that of *λ786*, the EcoRI insert of an isolated λgt11 cDNA clone. Clones *786*, *586*, and *407* are DraI–EcoRI deletions of λgt11 isolates while *119* is a PstI subclone derived from λ786. Clone *407Δ* is an AvaII-DraI deletion of 407 and *407T* was produced by PCR amplification of a novel 3′ sequence (see Materials and Methods). *A*, AvaII; *D*, DraI; *E*, EcoRI; *H*, HindIII; *P*, PstI; and asterisk, translation stop codon.

A battery of protease inhibitors was present in all these steps (Citi and Kendrick-Jones, 1986). After lysis of the bacterial cells and centrifugation to remove cellular debris, the proteins were precipitated from the supernatant by the addition of 5 vols of ethanol and stirred at 4°C for 30 min. A heavy, sticky precipitate formed which was resuspended in 10 ml (per liter of culture) of 25 mM Tris, pH 7.5, 1 mM $MgCl_2$, 1 mM DTT and then dialyzed against 2 × 2.5 liters of the same. Solid urea was added to 7 M to dissolve the precipitate which was fractionated on a DEAE-cellulose DE52 column (Whatman, Maidstone, UK) with a 0–500 mM NaCl gradient in 6 M urea, 25 mM Tris pH 7.5, 1 mM $MgCl_2$, and 1 mM DTT. Fractions containing the required polypeptides were identified by SDS-PAGE and checked by Western blotting. The fractions were pooled and dialyzed into 0.6 M NaCl, 25 mM sodium phosphate, pH 7.0, 10 mM Tris, pH 7.5, 0.5 mM sodium azide, and 2 mM DTT (myosin storage/dilution buffer) and stored at concentrations between 0.5 and 2 mg ml^{-1}. In later preparations all the expressed myosin fragments, with the exception of 119, were further purified by dialyzing into low salt buffer (50 mM NaCl, 25 mM sodium phosphate, pH 6.5, 5 mM $MgCl_2$ and 0.5 mM DTT) and collecting the precipitate by centrifugation at 30,000 *g* for 30 min before resuspending in storage/dilution buffer at 4–5 mg ml^{-1}.

Analysis of the Expressed Proteins

Sedimentation Analysis. Samples of the expressed myosin rod proteins (100 μl, 0.5 mg ml^{-1}) were dialyzed in small dialysis bags (visking dialysis tubing size 8/32) against a range of salt concentrations (50–400 mM NaCl) in 25 mM sodium phosphate, pH 7.5, 0.5 mM DTT, and 2 mM $MgCl_2$, (sedimentation buffer) for 5 h with gentle agitation. For critical concentration determinations a range of protein concentrations between 0.1 and 3.0 mg ml^{-1} were dialyzed against 150 mM NaCl in 'sedimentation buffer.' Dialyzed samples were weighed to determine final volume then centrifuged at 100,000 *g* for 20 min in a Beckman airfuge (Beckman Instruments Inc., Fullerton, CA). Previous sedimentation velocity measurements on thymus myosin filaments (Kendrick-Jones et al., 1987) indicated that any oligomers with sedimentation coefficients larger than 15S would be sedimented under these conditions (see also Pollard, 1982). The top 40% of each supernatant was taken for analysis by SDS-PAGE. The remainder of the supernatant was removed from the tube and the pellet redissolved in 100 μl of myosin storage/dilution buffer overnight at room temperature. Samples of the pellets were taken for SDS-PAGE. The solubility of the myosin rod fragments (expressed as percent fragment in the supernatant) were determined by measuring the relative amounts of each fragment in the pellet and supernatant fractions by densitometry of the stained PAGE gel bands using either a Camag electrophoresis densitometer (Cambridge Instruments, Cambridge, UK) or with a Molecular Dynamics Computing Densitometer (model 300A; Molecular Dynamics, Sunnyvale, CA).

Electron Microscopy

Samples for EM were prepared by a number of procedures: (*a*) Native and expressed myosin rod proteins (~0.5 mg ml^{-1}) in 600 mM NaCl, 40 mM Imidazole, pH 7.3, 5 mM $MgCl_2$ were rapidly diluted with 3 vols of water (final concentration 150 mM NaCl, 1 mM $MgCl_2$, 10 mM Imidazole, pH 7.3) and 10-μl aliquots taken for negative staining. Similar aggregates were formed if the proteins were dialyzed for 90 min against the 150 mM NaCl solution. (*b*) 10-μl aliquots of the samples from the sedimentation assays which had been dialyzed against 50 mM, 100 mM, and 150 mM NaCl in 2 mM $MgCl_2$, 25 mM phosphate buffer, pH 7.5, 0.5 mM DTT were taken for negative staining. (*c*) For paracrystal formation, 100-μl aliquots of native LMM, rod, and expressed fragments 786, 586, and 586ΔC (~0.5 mg ml^{-1}) were initially dialyzed against 50 mM Tris-HCl, pH 8.25, containing 50 mM potassium thiocyanate (KCNS) for native LMM, 100 mM KCNS for native rod, 65 mM KCNS for expressed fragments 786 and 586, and 0–80 mM KCNS for expressed 586ΔC. The solutions were centrifuged in an airfuge for 15 min at 30 psi (100,000 *g*) and then redialyzed against the appropriate Tris-HCl buffer/KCNS solution containing in addition 50 or 100 mM $CaCl_2$ (or other divalent cations) to form the paracrystals.

For negative staining 10-μl samples were applied onto carbon coated, 400 mesh grids and left for 15 s. The grids were washed with six drops of the appropriate salt/buffer solution and stained with six drops of 1.5% uranyl acetate and dried. For shadowing, the samples were mixed with an equal volume of glycerol, sprayed onto freshly cleaved mica, and shadowed with platinum and carbon (Citi and Kendrick-Jones, 1987a). The specimens were examined in a Philips electron microscope (model EM400; Philips Electronic Instruments Co., Mahwah, NJ) operated at 80 kV and representative views photographed.

Results

Shotgun sequencing of the longest of our cDNA clones (λ786) yielded data which agrees almost completely with the sequence already published by Shohet et al. (1989). The only difference is that in their deduced protein sequence there is a disruption in the heptad and 28-residue repeat patterns in zone 39 of the rod, whereas in our translated cDNA sequence we detected an extra amino acid residue in this region. In our sequence there is no disruption in the repeats and the protein sequence is identical to that of human nonmuscle myosin reported by Saez et al. (1990). The DNA in this region was found to be subject to compressions when electrophoresed on the sequencing gel such that the sequence reported as: CGA GCC AAC GTC CGC AGG (bases 5662-5679, protein sequence: RANVRR, Shohet et al., 1989), we have read as: CGA GCC AAC GCG TCC CGC AGG (RANASRR). Some of our clones have a longer 3′ untranslated region to those described by Shohet et al. (1989) and terminate in a short poly-A tail preceded by a putative poly-A addition signal (data not shown). This would suggest a 3′ untranslated region of some 1.4 kb.

Table I. SDS-PAGE and Western Blot Analysis of the Expressed Rod Fragments

Clone name	Predicted size	Estimated size	BM1	BM4	BM3
	kD	*kD*			
786	91.0	88.2	+	+	+
586	68.2	70.6	+	+	+
407	47.2	50.4	−	+	+
119	13.7	14.4	−	+	+
786Δ	87.5	82.1	+	+	+
586Δ	64.7	67.2	+	+	+
407Δ	43.8	43.4	−	+	+
407T	45.8	46.8	ND	+	ND

mAb BM1 binds to a region ~71 nm from the COOH-terminal end of brush border myosin, whereas the epitopes for antibodies BM3 and BM4 are at the COOH terminus of the molecule (Citi and Kendrick-Jones, 1987*b*). BM1 and BM4 are IgGs, whereas BM3 is an IgM.

Expression and Characterization of the Expressed Proteins

The cDNA expression clone 786 codes for a protein of 786 amino acids with a predicted molecular weight of 91,000 daltons, which is in good agreement with its size estimated from SDS-PAGE (Table I). Aligning the sequence with that of chicken smooth muscle MHC (Yanagisawa et al., 1987) indicates that it codes for more than two thirds of the rod region (from residue 1,180 to the COOH-terminus).

Using our sequence data we designed a number of expression constructs using pINII expression vectors (Nakamura and Inouye, 1982). Two types of constructs were made: those with deletions at the 5′ end of the sequence to generate deletion mutants 786, 586, 407, etc. and those with deletions at the extreme 3′ end of the coding sequence, which remove or truncate the nonhelical COOH-terminal tailpiece, hence clone 407 becomes 407Δ or 407T (Fig. 2). The constructs were expressed and after initial screening by SDS-PAGE, the required expressed proteins were purified using procedures based on the known stability properties of native myosin rod and LMM. Proteins made in this way were stable to ethanol and heat, selectively precipitated at low pH and pI and showed mobilities on PAGE gels close to those predicted (Fig. 3, Table I). The appearance of multiple bands in the expressed protein samples was noted from the outset of the purification procedure despite the presence of 10 mM EDTA and a wide spectrum of protease inhibitors (Citi and Kendrick-Jones, 1986). They were not removed by chromatography or by repeated low salt precipitation cycles. Preliminary data indicates that nicking of the coiled coil occurs at the amino terminus and the extra bands have no effect on the sedimentation assays or on the formation of paracrystals. Under nondissociating conditions on glycerol-PAGE (40% glycerol/7.5% acrylamide) in the presence of 40 mM sodium pyrophosphate the samples run as single bands (Fig. 3*B*). Thus the multiple bands are not apparent until the proteins are boiled in SDS loading buffer for the SDS-PAGE analysis.

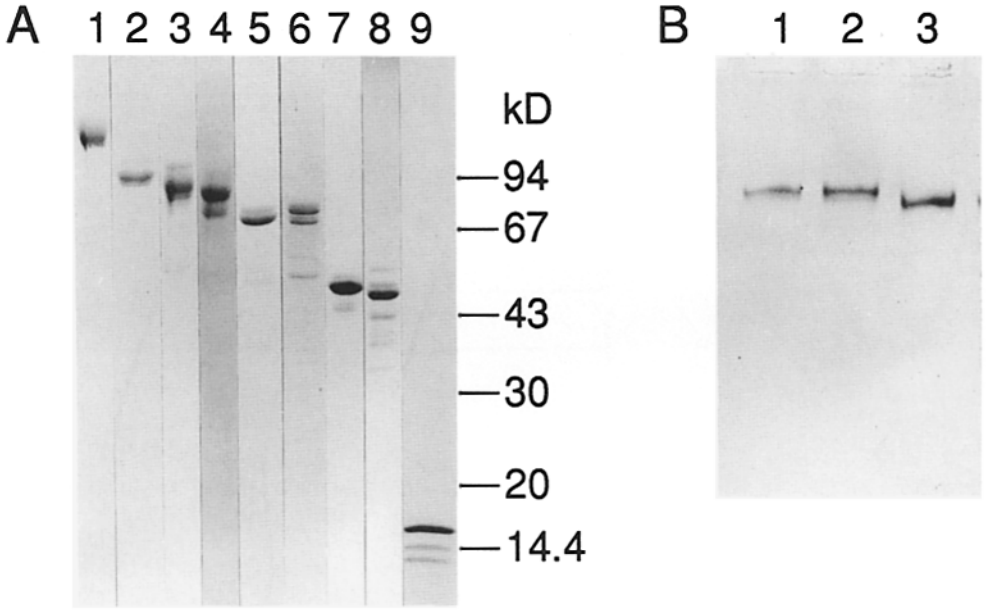

Figure 3. PAGE analysis of expressed rod fragments. (*A*) SDS-PAGE. Lane *1*, Isolated chicken gizzard myosin rod (proteolytic digest); lane *2*, isolated gizzard light meromyosin (digest); lane *3*, expressed myosin fragment 786; lane *4*, fragment 786Δ; lane *5*, fragment 586; lane *6*, fragment 586Δ; lane *7*, fragment 407; lane *8*, fragment 407Δ; and lane *9*, fragment 119. See Table I for details of predicted and observed fragment size. (*B*) Glycerol-PAGE. Lane *1*, fragment 407; lane *2*, fragment 407T; and lane *3*, fragment 407Δ.

The proteins were further tested with the brush border myosin rod mAbs BM1, BM3, and BM4 (Citi and Kendrick-Jones, 1987*b*), to check their identity and their approximate lengths (Table I). Earlier work (Citi and Kendrick-Jones, 1987*b*) had suggested that BM4 bound to the extreme COOH-terminal end of the rod but our results show it still binds to rod molecules where the last 35 residues have been deleted. Rotary shadowing the expressed proteins revealed rod-like structures of the correct average size in the electron microscope. Furthermore low angle x-ray scattering analysis (carried out by Dr. W. Faruqi, LMB, Cambridge, UK) on these proteins yielded data consistent with α-helical coiled-coil rods (data not shown).

Assembly Properties of the Nonmuscle Myosin Fragments

Sedimentation Assay. All the expressed fragments with the exception of fragment 119, showed assembly characteristics which were similar, i.e., they assembled into polymers at low salt and as the salt concentration was increased they disassembled and became soluble monomers (>300 mM) (Fig. 4 *a*). The effect of lowering the pH from 7.5 to 6.5 on the assembly of all the fragments was minimal. Fragment 119 however was soluble under all conditions tested, i.e., at all salt concentrations and at pH 6.5 and 7.5. It even remained completely soluble when mixed with equal concentrations of fragments 586 or 407 in high salt and dialyzed to low salt at pH 6.5, conditions under which fragments 586 and 407 readily assembled (data not shown). O'Halloran et al., 1990 have previously shown that a minimum length of rod is required for *Dictyostelium* myosin filament assembly. The results with 119 suggest a minimum rod length is also required for assembly of vertebrate nonmuscle myosins. Rod paracrystals assembled from COOH-terminally intact material have a 14.3-nm repeat which indicates that their constituent molecules are staggered by this amount. If this is indeed the case, then it is not surprising that rod fragment 119 did not assemble, since after taking into account the 35-residue tailpiece it is <14.3 nm long (14.3 nm of α-helix corresponds to ~98 residues, i.e., 0.1485-nm rise per amino acid residue [McLachlan and Karn, 1982]) Low angle x-ray scattering analysis on 119 confirms that it is the correct size and shape to be a short piece of coiled coil (A. R. Faruqi, unpublished data). Hence its inability to assemble is unlikely to be due to incorrect formation of the α-helical coiled-coil structure.

Deletions at the COOH-terminus lead to a dramatic alteration in the assembly properties of the rod fragments (Fig. 4 *b*). Removal of the entire 35-residue COOH-terminal tailpiece results in a clear shift in the solubility curves, so that at 150 mM NaCl >60% of the protein remained soluble. This change in solubility is because of a dramatic increase in the critical rod fragment concentration (C_c) required for assembly (Fig. 4 *c*). At 150 mM NaCl, pH 7.5, deletion of the COOH-terminal tailpiece leads to a 20–50-fold increase in critical concentration (C_c); from C_c ~20–50 μg ml^{-1} for the rod with an intact or truncated COOH terminus to ~1 mg/ml^{-1} for the deleted COOH-terminal (CΔ) fragments. Unlike fragment 119 which is assembly incompetent, the CΔ fragments could be forced to assemble at higher protein or at lower salt concentrations. The data indicate that the action of the tailpiece is to cause self-assembly to occur at protein concentrations considerably below those at which it would otherwise occur. This observation is consistent with the idea that the nonhelical tailpiece in some way promotes assembly, rather than being absolutely required for assembly.

Coassembly experiments. The finding that the intact and deleted COOH-terminal fragments have very different critical concentrations for assembly suggests either that the tailpiece accelerates a step or steps in the assembly pathway, or else it induces assembly to occur via a different pathway. As one way to distinguish between these possibilities, the following coassembly experiments were carried out (Fig. 5). When the intact COOH-terminal fragments 586 and 407 were mixed together at a 1:1 ratio, assembly of both of them was increased, i.e., less of each of them was present in the supernatants after dialysis and centrifugation. In contrast, when fragment 586 was mixed with the COOH-terminal-deleted fragment 407Δ in a similar ratio, then assembly of 586 and 407Δ was not significantly altered, i.e., fragment

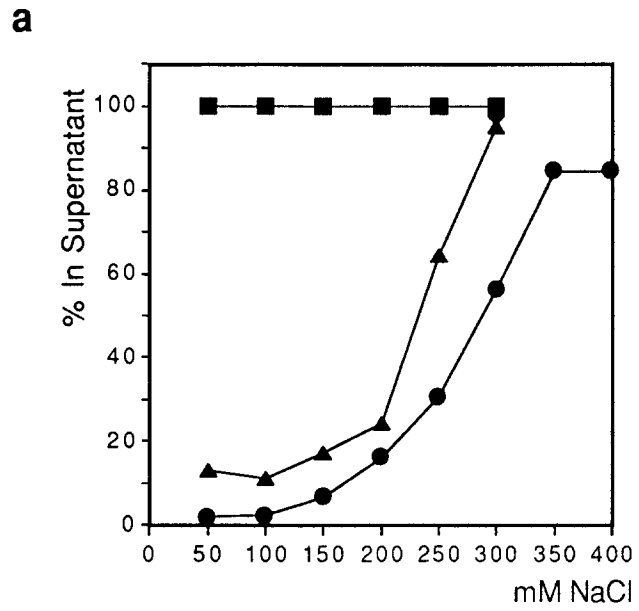

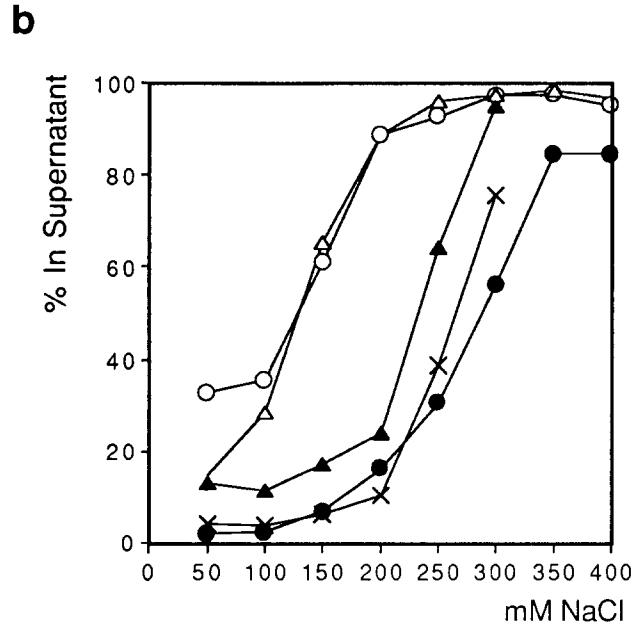

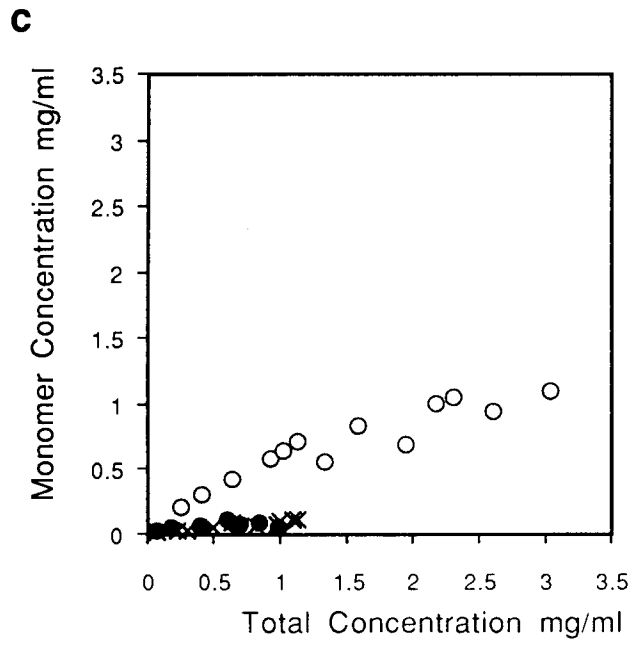

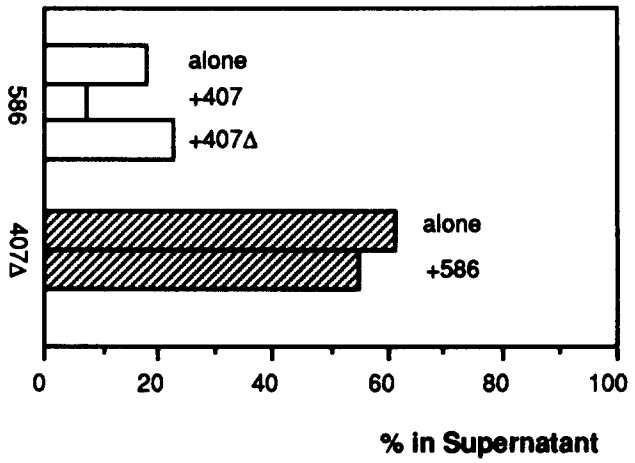

Figure 5. Coassembly of myosin rod fragments. Mixtures of equal concentrations of *586 alone* or with either *407* or *407Δ*, or *407Δ alone* or with *586* (total protein concentration 0.5 mg/ml^{-1}) were dialyzed against sedimentation buffer at 150 mM NaCl, centrifuged and the supernatant and pellet fractions analyzed by SDS-PAGE. The bar graphs are grouped according to the fragment whose solubility was measured and any other fragment present in the dialysis bag is shown after the bar. The lower solubility of *586* in the presence of *407* suggests some cooperative effect on filament formation. The minimal effect of *586* on the solubility of *407Δ* shows that intact molecules are unable to 'rescue' COOH-terminal deleted molecules. Identical results were obtained at 200 mM NaCl and when other mixtures of intact and COOH-terminal deleted rod fragments were used.

407Δ still remained mainly soluble. Thus, fragment 586 with an intact COOH-terminal tailpiece is not able to 'rescue' the COOH-terminal-deleted fragment 407Δ by interacting with it to assemble into copolymers. There is apparently a requirement for symmetry in the self-assembly process, suggesting that the growing polymer senses in some way whether incoming molecules have the COOH-terminal tailpiece or not. This is consistent with earlier work with proteolytic rod fragments (Cross and Vanderkerckhove, 1986), which indicated that a mixture of chicken gizzard LMM fragments with intact and deleted COOH-termini segregated to the pellet

Figure 4. The assembly properties of the expressed myosin rod fragments. (*a*) The assembly behavior of expressed fragments 586 (−▲−), 407 (−●−), and 119 (−■−) as a function of the salt concentration. At these protein concentrations (0.5 mg ml^{-1}) all the fragments including 786 (not shown) show similar assembly profiles with the exception of fragment 119 which is completely soluble. (*b*) Comparison of the assembly behavior of expressed fragments with the COOH-terminal tailpiece (407 [−●−] and 586 [−▲−]) and without the COOH-terminal tailpiece (407Δ [−○−] and 586Δ [−△−]) as a function of the salt concentration. Deletion of the COOH-terminal tailpiece increases the solubility of fragments 407 and 586. 407T (X) (last 15 amino acids deleted). (*c*) The critical monomer concentration for assembly of fragment 407 (●), 407Δ (○) and 407T (X) (last 15 amino acids deleted) at 150 mM NaCl, 2 mM $MgCl_2$, pH 7.5. The change in solubility brought about by deletion of the tailpiece is due to a dramatic increase in the critical monomer concentration required for assembly.

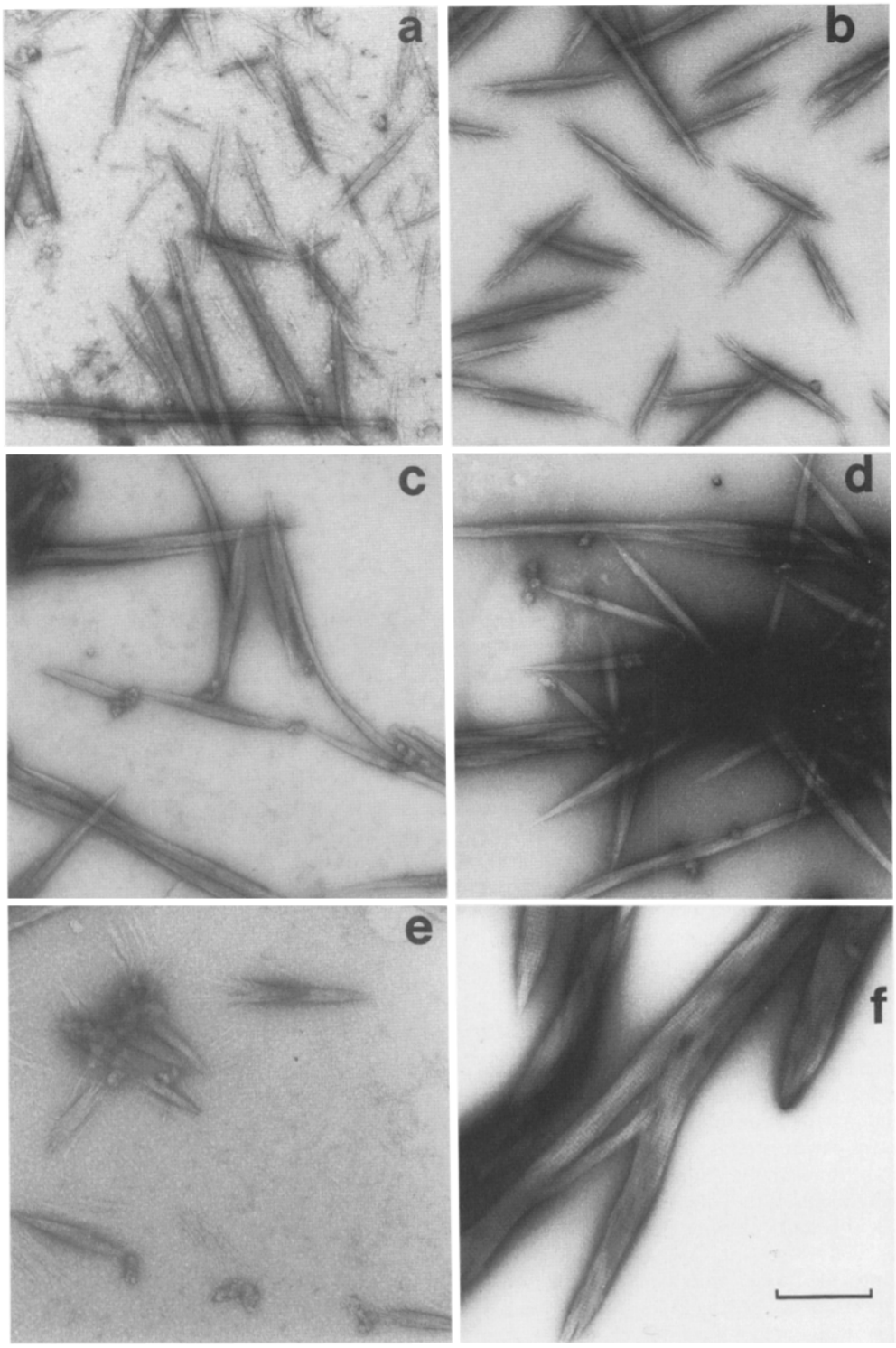

Figure 6. Electron micrographs of the ordered aggregates formed by native and expressed myosin rod fragments at approximately physiological salt, pH, and $MgCl_2$ concentrations (150 mM NaCl, 1 mM $MgCl_2$ and pH 7.3). (*a*) expressed 786; (*b*) native myosin rod; (*c*) native myosin LMM; (*d*) expressed 586; (*e*) expressed 586Δ at ~0.5 mg ml^{-1}; (*f*) expressed 586Δ (at >1.0 mg ml^{-1}) left for ~16 h. Fragments 786 and 586 (and fragment 407 not shown) form structures very much like those formed by the native rod and LMM control fragments. Deletion of the nonhelical tailpiece disrupts formation of these needle-like structures. However, close examination of *e* reveals numerous small parallel aggregates in the background. By increasing the protein concentrations of these COOH-terminal deleted fragments, they will, given time, form large well ordered structures with prominent 14.3-nm periodicities as seen in *f*. Note the conditions used were similar to those used in the sedimentation assay (at 150 mM NaCl) shown in Fig. 4. All the 'aggregates' were formed by the rapid dilution from high salt into low salt buffer procedure. Very similar structures were observed when the rod fragments were dialyzed into the low salt buffer conditions or samples were taken directly from the sedimentation assay. The results are very reproducible with different preparations of the rod fragments. The micrographs shown are representative of all the material observed on the grids. Bar, 0.1 μm.

and supernatant fractions, respectively, after ultracentrifugation. These results mean that provision of nuclei composed of intact, assembly competent rod molecules does not allow molecules with deleted COOH-termini to coassemble, indicating that the nonhelical COOH-terminus promotes both polymer initiation and polymer growth.

Electron Microscopy. The ability of the expressed fragments to assemble was compared by examining the assembled forms in the electron microscope after negative staining (Fig. 6). Under approximately physiological conditions (150 mM NaCl, 2 mM $MgCl_2$, pH 7.3) the expressed fragments 586 and 786 assembled to form numerous short symmetrical filaments with pointed ends (Fig. 6, *a* and *d*) which were very similar to those formed by the native rod and LMM fragments (Fig. 6, *b* and *c*). Fragment 786 showed a slightly elevated solubility in the sedimentation assay (data not shown) but formed filaments which were similar in structure although variable in size compared with those formed by the other fragments. Under the same conditions the COOH-terminal-deleted fragment 586Δ formed only a few small

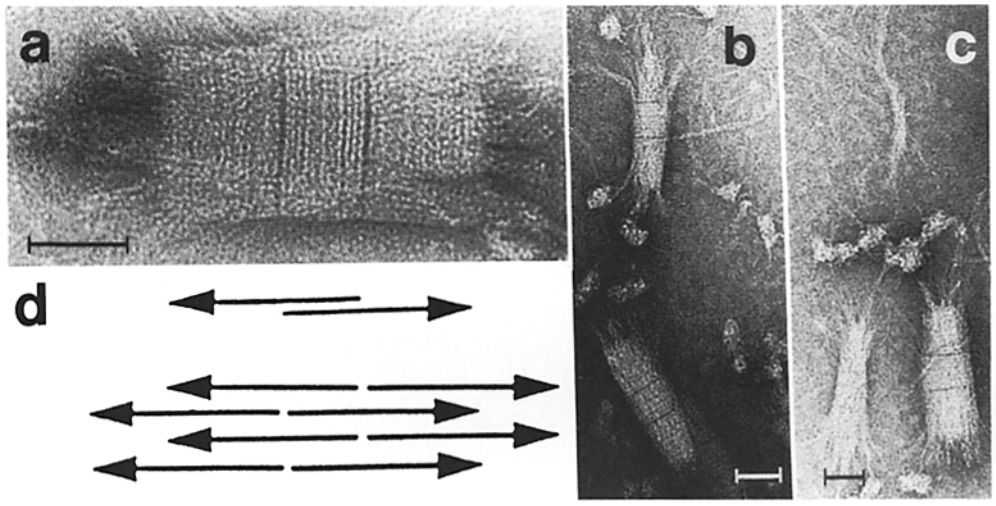

Figure 7. Electron micrographs of paracrystalline 'segments' formed by native and expressed rod fragments. (*a*) native gizzard LMM; (*b*) expressed 786 fragment; (*c*) expressed 586 fragment; and (*d*) schematic representation of the packing of the rod molecules in the 'segments' as proposed by Kendrick-Jones et al., (1971). The 'segments' display both bipolar and polar bonding patterns with an axial stagger of 43 nm. The NH_2-terminal ends of the molecules are indicated by the arrowheads and the dark staining lines on each side of the central 43-nm region are believed to represent small gaps between the molecules, i.e., they are not end to end bonded. The lengths of the molecules estimated from the micrographs are in agreement with the expected values, i.e., ~100 nm for the native LMM, ~110 nm for 786, and ~90 nm for 586. Bars, 50 nm.

"carrot-shaped" arrays and a high concentration of protein was evident in the background (Fig. 6 *e*). When higher concentrations of 586Δ (>1 mg/ml^{-1}) were used and the samples were left for ~16 h at 4°C, then the small loosely packed arrays aggregated to form large paracrystalline structures with prominent 14.3-nm periodicities (Fig. 6 *f*). The formation of these large aggregates which require high protein concentrations and time suggests that they assemble by a less favorable pathway with few stable nuclei and a slow filament growth rate.

To further probe the interactions involved in assembly, attempts were made to induce the expressed fragments to form paracrystalline segments in the presence of high concentrations of divalent cations (Fig. 7). As previously demonstrated (Kendrick-Jones et al., 1971) native LMM readily forms these bipolar segments where the molecules are staggered by 43 nm as shown in Fig. 7 *d*. Under similar conditions, fragments 786 and 586 formed similar structures although the number observed were few and they tended to be less well ordered and rather ragged. We were unable to induce the 586Δ fragment to form such paracrystalline arrays despite testing a variety of conditions, for example, differing pHs from 7.5 to 8.6, using differing amounts of the solubilizing agents potassium thiocyanate and sodium chloride and different divalent cations such as Ca^{2+}, Mg^{2+}, or Cd^{2+} at high concentrations. These results provide further proof that the COOH-terminal tailpiece is crucial for generating bipolar assemblies with a 43-nm stagger which may reflect one of the axial staggers between myosin rods involved in assembling thick filaments.

In both the segments and filament aggregates the electron-dense striations in the assemblies are due to stain accumulation at the ends of the molecules. Hence the COOH-terminal nonhelical domain enhances the assembly of rod fragments into two types of polymers having two different molecular overlaps. One can therefore exclude that the tailpiece recognizes and binds to a single target site on a neighboring molecule. We note further that filaments formed from rod fragments with intact COOH termini and (at higher concentrations) those with deleted COOH termini both have 14.3 nm striations, suggesting that the tailpiece does not alter the overlap between molecules in the filaments. It remains possible however that two or more recognition sites for the tailpiece exist on neighboring molecules. To test this possibility we made further truncations in the tailpiece region, and assayed the assembly of the resulting constructs (Fig. 4 *b*). Truncation of the brush border myosin tailpiece sequence down to 40% of its original length (407T) did not affect its function, again consistent with there being no specific sequence requirements in this region. This truncation removes the last 15 amino acids and most of the region of negative charge within the tailpiece (Fig. 1), yet it does not appear to affect the assembly of the rod fragments.

Discussion

The most significant difference between the α-helical coiled coil rod regions of vertebrate smooth muscle/nonmuscle and sarcomeric (skeletal) muscle myosins is the presence in the former of nonhelical carboxyl-terminal tailpieces, ~35–43 amino acids long (Fig. 1). Although the lengths and sequences of the COOH-terminal tailpieces vary in the different smooth muscle/nonmuscle myosins, the distribution of hydrophobic, basic, and acidic amino acids is preserved (Fig. 1). It is not clear from the sequences however whether the conformation of the tailpiece is a true random coil or whether some nonhelical secondary structure is present.

Previous experiments involving the removal of this COOH-terminal nonhelical domain from various myosins, either by proteolysis or site-directed mutagenesis (Cross and Vanderkerckhove, 1986; Sinard et al., 1990; Ikebe et al., 1991) have suggested that this domain is required for self-assembly. In addition work on chicken epithelial brush border myosin (Citi and Kendrick-Jones, 1988) showed that mAbs binding to the COOH-terminal tip of the rod blocked filament assembly while those binding to regions one third and two thirds along the rod, gave rise to assembly intermediates, suggesting that some interaction involving the

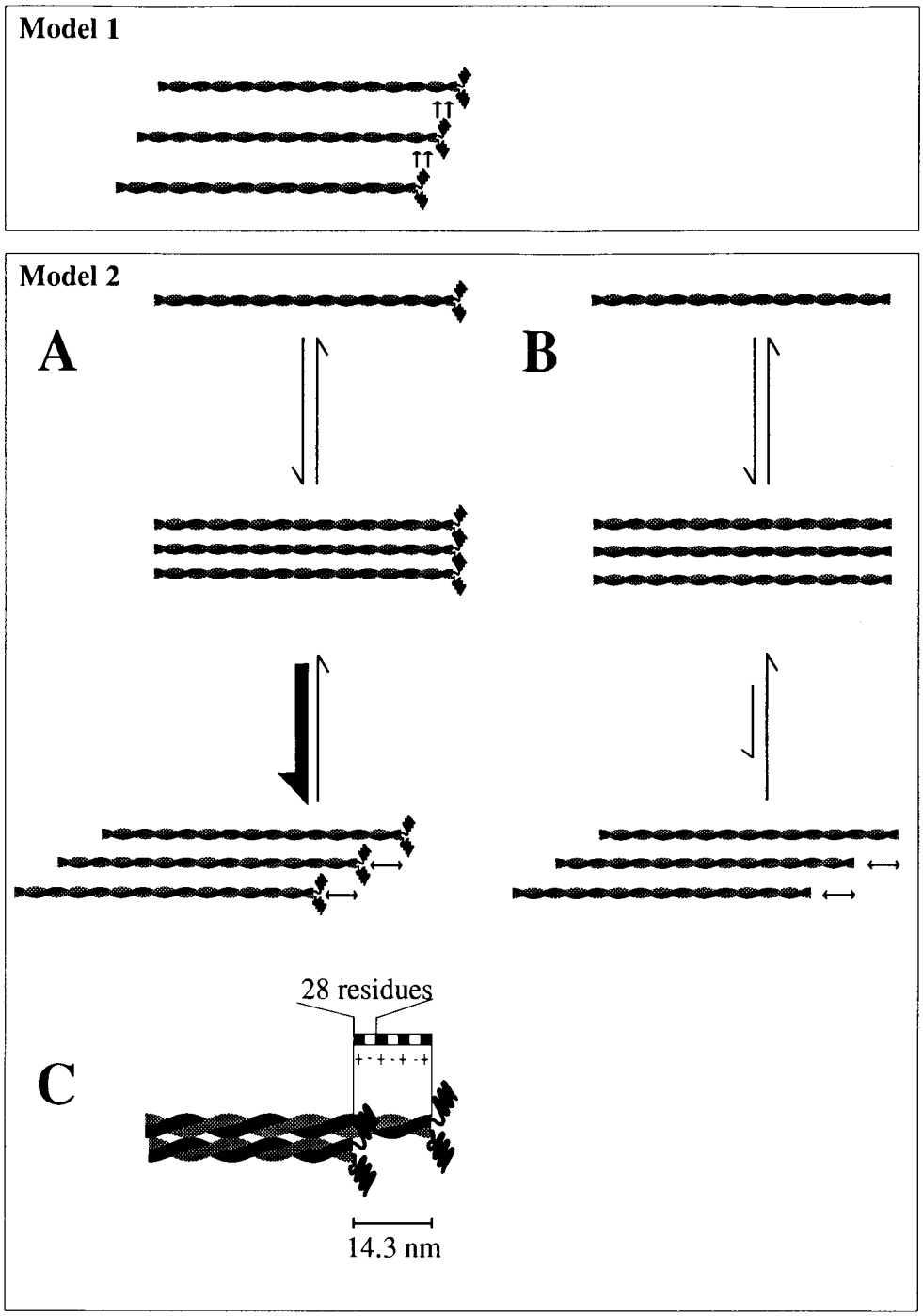

Figure 8. Models to explain the action of the nonhelical tailpiece on the assembly of smooth and nonmuscle myosins. In *Model 1*, the tailpiece promotes assembly by binding to a target site on a neighboring molecule. Molecular overlaps are specified by this site-specific binding. In *Model 2*, the tailpieces of neighboring molecules clash, forcing an intermolecular stagger to occur and thus when tailpieces are present, unstaggered modes of assembly are disfavored (A). This model supposes that in the absence of tailpiece, unstaggered intermediates accumulate (B), which only infrequently develop productive staggers and go on to assemble into filaments. This model makes a testable prediction, that unproductive oligomers of tailpiece-free molecules should be present under assembly conditions. Preliminary observations are in agreement with this prediction (see material in background of Fig. 6 *e*). The result of productive filament assembly (A) is seen in the electron microscope as repeating striations of 14.3 nm which represent 98 residues of α-helical coiled coil or 3.5 repeating charge units (*C*). Packing of rod molecules into filaments is thought to be determined by a unit of 7 × 28 residue repeats (196 amino acids), half staggered relative to each other resulting in a 14.3-nm repeating structure, i.e., 196/2 × 0.1485 nm rise/amino acid (Quinlan and Stewart, 1987).

nonhelical tailpiece is a primary step in filament assembly. Antibodies to *Acanthamoeba* and *Dictyostelium* myosin IIs have similarly demonstrated the importance of the distal tail in the initial steps in the assembly of these myosins (Pagh and Gerisch, 1986; Rimm et al., 1990). Recently Ikebe et al. (1991) made the interesting observation that after assembly of vertebrate smooth muscle myosin filaments, the tailpiece can be proteolytically cleaved away, without inducing filament disassembly. The present series of experiments were designed to address the question of which steps in the assembly pathway of a vertebrate nonmuscle myosin are promoted by the presence of the tailpiece.

Models to Explain the Role of the Tailpiece

We have considered two types of possible model to explain our results (Fig. 8). Both postulate that the tailpiece produces its effect on the critical monomer concentration for assembly by enhancing the ability of molecules to bind productively to one or more partners in such a way that the molecules build into a filament. In Fig. 8, *Model 1*, the tailpiece is postulated to recognize and bind to a target site on one or more neighboring molecules, thereby increasing the binding constant, and specifying a particular overlap between molecules. This was suggested by E. D. Korn and his col-

leagues to be the way in which the COOH terminus of *Acanthamoeba* myosin II promoted myosin filament assembly (Atkinson et al., 1989). Recently Kalbitzer et al. (1991) showed by nuclear magnetic resonance spectroscopy that even the COOH terminus of rabbit skeletal muscle myosin contains a short unfolded mobile region which they propose might function as a 'kind of cement' to stabilize the thick filament structure. In Fig. 8, *Model 2*, the nonhelical tailpiece is postulated to block an otherwise dominant, but unproductive mode of intermolecular binding (Fig. 8 *A*). In this model the tailpiece promotes assembly by diverting molecules out of this futile cycle, and on to a productive pathway.

The lack of any obvious sequence anomaly within the rod, which would indicate a specific binding site, argues against Fig. 8, *Model 1*. The finding that the tailpiece enhances both filament and segment assembly, and hence enhances two different molecular overlaps, also argues against a specific single binding site in the myosin rod. Finally, we found that the tailpiece could be deleted down to half its wild type length, substantially altering its charge, without affecting function. This again renders it unlikely that specific sequence features in the tailpiece are required for function. Rather, the data indicate that the COOH-terminal tailpiece must have a minimum size, but that its length and sequence can vary substantially without affecting function (see Fig. 1). We feel this is much more consistent with a steric blocking role (model 2) than with there being one or more specific tailpiece-binding sites within the rod molecule. Further support is provided by the observations of Ikebe et al. (1991) that the tailpiece can be selectively removed from myosin filaments by proteolytic cleavage without inducing filament disassembly, indicating that it is accessible and not buried in the spaces in the filament structure.

For a steric blocking mechanism to be effective in promoting productive assembly, there must be at least one competing, unproductive pathway, which sequesters molecules lacking a tailpiece. Our experiments do not reveal details of this competing pathway, but it might for example involve rod molecules lacking a COOH-terminal nonhelical tailpiece tending to bind to one another with full overlap (see Fig. 8 *B*). The model requires that this mode of assembly becomes unstable after the addition of a few molecules. Steric interference by the tailpieces with one another would force a stagger to occur between molecules, thereby promoting productive filament assembly. In this model, myosin rod fragments without tailpiece would interact rapidly to form small aggregates, possibly only dimers or trimers, which once formed are able only slowly to reorganize (dissociate or slip) to form protofilaments. The action of the tailpiece would be to promote this reorganization. In this connection, it is interesting to note that Egelhoff et al. (1991) have demonstrated that a COOH-terminal tailpiece promotes the disassembly of *Dictyostelium* myosin filaments.

In conclusion, we have shown that the COOH-terminal nonhelical tailpiece of a vertebrate nonmuscle myosin II acts to lower the critical concentration of myosin required for assembly by 20–50-fold at physiological ionic strength and have presented evidence consistent with a role for this tailpiece in the steric blocking of unproductive modes of assembly. By extending the approach described, it should now be possible to dissect in molecular detail those steps of the assembly reaction which are promoted by the presence of the tailpiece.

Received for publication 28 January 1992 and in revised form 25 May 1992.

References

Atkinson, S. J., and M. Stewart. 1991. Expression in *Escherichia coli* of fragments of the coiled-coil rod domain for rabbit myosin: influence of different regions of the molecule on aggregation and paracrystal formation. *J. Cell Sci.* 99:823–836.

Atkinson, M. A. L., P. K. Lambooy, and E. D. Korn. 1989. Cooperative dependence of the actin activated Mg^{2+}-ATPase activity of *Acanthamoeba* myosin II on the extent of filament phosphorylation. *J. Biol. Chem.* 264:4127–4132.

Babij, P., and M. Periasamy. 1989. Myosin heavy chain isoform diversity in smooth muscle is produced by differential RNA processing. *J. Mol. Biol.* 210:673–679.

Bunnell, B. A., and V. J. Kidd. 1989. Formation of deletion mutants by polymerase chain reaction. *Technique (Phila.)* 1(2):103–107.

Burnette, W. N. 1981. "Western blotting": electrophoretic transfer of proteins from SDS-PAGE to unmodified nitrocellulose and radiographic detection with antibody and radioiodinated protein A. *Anal. Biochem.* 112:195–203.

Citi, S., and J. Kendrick-Jones. 1986. Regulation *in vitro* of brush border myosin by light chain phosphorylation. *J. Mol. Biol.* 188:369–382.

Citi, S., and J. Kendrick-Jones. 1987*a*. Regulation of nonmuscle myosin structure and function. *Bioessays.* 7:155–159.

Citi, S., and J. Kendrick-Jones. 1987*b*. Studies on the structure and conformation of brush border myosin using monoclonal antibodies. *Eur. J. Biochem.* 165:315–325.

Citi, S., and J. Kendrick-Jones. 1988. Brush border myosin filament assembly and interaction with actin investigated with monoclonal antibodies. *J. Muscle Res. Cell Motil.* 9:306–319.

Cohen, C., and A. D. Parry. 1990. α-Helical coiled coils and bundles: how to design an α-helical protein. *Proteins Struct. Funct. Genet.* 7:1–15.

Craig, R., and J. Megerman. 1977. Assembly of smooth muscle myosin into side-polar filaments. *J. Cell Biol.* 75:990–996.

Craig, R., R. Smith, and J. Kendrick-Jones. 1983. Light chain phosphorylation controls the conformation of vertebrate nonmuscle and smooth muscle myosin molecules. *Nature (Lond.).* 302:436–439.

Cross, R. A., and J. Vanderkerckhove. 1986. Solubility-determining domain of smooth muscle myosin rod. *FEBS (Fed. Eur. Biochem. Soc.) Lett.* 200:355–360.

Cross, R. A., M. A. Geeves, and J. Kendrick-Jones. 1991. A nucleation-elongation mechanism for the self-assembly of side polar sheets of smooth muscle myosin. *EMBO (Eur. Mol. Biol. Organ.) J.* 10:747–756.

Davis, J. S. 1988. Assembly processes in vertebrate skeletal thick filament formation. *Annu. Rev. Biophys. Biophys. Chem.* 17:217–239.

Dibb, N. J., S. L. Brown, J. Karn, D. G. Moerman, S. L. Bolten, and R. H. Waterston. 1985. Sequence analysis of mutations that affect the synthesis, assembly and enzymatic activity of the *unc*-54 myosin heavy chain of *Caenorhabditis elegans. J. Mol. Biol.* 183:543–551.

Dibb, N. J., I. Maruyama, M. Krause, and J. Karn. 1989. Sequence analysis of the complete *Caenorhabditis elegans* myosin heavy chain gene family. *J. Mol. Biol.* 205:603–613.

Egelhoff, T. T., S. S. Brown, and J. A. Spudich. 1991. Spatial and temporal control of nonmuscle myosin localization: Identification of a domain that is necessary for myosin filament disassembly in vivo. *J. Cell Biol.* 112:677–688.

Ganguly, C., M. A. L. Atkinson, A. K. Attri, V. Sathyamoorphy, B. Bowers, and E. D. Korn. 1990. Regulation of the actin activated ATPase activity of *Acanthamoeba* myosin II by copolymerisation with phosphorylated and dephosphorylated peptides derived from the C-terminal end of the heavy chain. *J. Biol. Chem.* 265:9993–9998.

Harrington, W. F., and M. E. Rogers. 1984. Myosin. *Annu. Rev. Biochem.* 53:35–73.

Hinssen, H., J. D'Haese, J. V. Small, and A. Sobieszek. 1978. Mode of filament assembly of myosins from muscle and non-muscle cells. *J. Ultrastruc. Res.* 64:282–302.

Huynh, T. U., R. A. Young, and R. W. Davis. 1985. Construction and screening cDNA libraries in lambda gt 10 and lambda gt 11. *In* DNA Cloning Techniques: A Practical Approach. D. Glover, editor. IRL Press Ltd., Oxford. 49–78.

Ikebe, M., T. E. Hewett, A. F. Martin, M. Chen, and D. J. Hartshorne. 1991. Cleavage of a smooth muscle myosin heavy chain near its C-Terminus by α-Chymotrypsin. *J. Biol. Chem.* 266:7030–7036.

Josephs, R., and W. F. Harrington. 1968. Polymerisation of myosin filaments. *Biochemistry.* 7:2834–2847.

Kalbitzer, H. R., K. Maeda, A. Rösch, Y. Maeda, M. Geyer, W. Beneicke, J-P. Neidig, and A. Wittinghofer. 1991. C terminal structure and mobility of rabbit skeletal muscle light meromyosin as studied by one- and two-dimensional ^1H NMR spectroscopy and X-ray small-angle scattering. *Biochemistry.* 30:8083–8091.

Kelley, C. A., S. Kawamoto, M. A. Conti, and R. A. Adelstein. 1991. Phosphorylation of vertebrate smooth muscle and nonmuscle myosin heavy chains *in vitro* and in intact cells. *J. Cell. Sci. Suppl.* 14:49–54.

Kendrick-Jones, J., A. G. Szent-Györgyi, and C. Cohen. 1971. Segments from smooth muscle myosin rod. *J. Mol. Biol.* 59:527–529

Kendrick-Jones, J., W. Z. Cande, P. J. Tooth, R. C. Smith, and J. M. Scholey. 1983. Studies on the effect of phosphorylation of the 20,000 Mr light chain of vertebrate smooth muscle myosin. *J. Mol. Biol.* 165:139–162.

Kendrick-Jones, J., R. C. Smith, R. Craig, and S. Citi. 1987. Polymerisation of vertebrate nonmuscle and smooth muscle myosins. *J. Mol. Biol.* 198:241–255.

Ketchum, A. S., C. T. Stewart, M. Stewart, and D. P. Kiehart. 1990. Complete sequence of the *Drosophila* nonmuscle myosin heavy chain transcript: conserved sequences in the myosin tail and differential splicing in the 5′ untranslated sequence. *Proc. Natl. Acad. Sci. USA.* 87:6316–6320.

Maeda, K., A. Rösch, Y. Maeda, H. R. Kalbitzer, and A. Wittinghofer. 1991. Rabbit skeletal muscle myosin. Unfolded carboxyl-terminus and its role in molecular assembly. *FEBS (Fed. Eur. Biochem. Soc.) Lett.* 281:23–26.

Matsudaira, P. T., and D. R. Burgess. 1978. SDS microslab linear gradient polyacrylamide gel electrophoresis. *Anal. Biochem.* 87:386–396.

McLachlan, A. D. 1984. Structural implications of the myosin amino acid sequence. *Annu. Rev. Biophys. Biophys. Chem.* 13:167–189.

McLachlan, A. D., and J. Karn. 1982. Charge distributions in the myosin rod amino basic sequence match crossbridge spacings in muscle. *Nature (Lond.).* 299:226–231.

Megerman, J., and S. Lowey. 1981. Polymerisation of myosin from smooth muscle of calf aorta. *Biochemistry.* 20:2099–2110.

Molina, M. I., K. E. Kropp, J. Gulick, and J. Robbins. 1987. The sequence of an embryonic myosin heavy chain gene and isolation of its corresponding cDNA. *J. Biol. Chem.* 262:6478–6488.

Nagai, R., D. M. Larson, and M. Periasamy. 1988. Characterization of a mammalian smooth muscle myosin heavy chain cDNA clone and its expression in various smooth muscle types. *Proc. Natl. Acad. Sci. USA.* 85:1047–1051.

Nakamura, K., and M. Inouye. 1982. Construction of versatile expression cloning vehicles using the lipoprotein gene of *Escherichia coli*. *EMBO (Eur. Mol. Biol. Organ.) J.* 1(6):771–775.

O'Halloran, T., S. Ravid, and J. A. Spudich. 1990. Expression of *Dictyostelium* myosin tail segments in *Escherichia coli*: domains required for assembly and phosphorylation. *J. Cell Biol.* 110:63–70.

Pagh, K., and G. Gerisch. 1986. Monoclonal antibodies binding to the tail of *Dictyostelium discoideum* myosin: their effects on antiparallel and parallel assembly and actin activated ATPase activity. *J. Cell Biol.* 103:1527–1538.

Pollard, T. D. 1982. Structure and polymerization of *Acanthamoeba* myosin II filaments. *J. Cell Biol.* 95:816–825.

Quinlan, R. A., and M. Stewart. 1987. Crystalline tubes of myosin subfragment-2 showing the coiled-coil and molecular interaction geometry. *J. Cell Biol.* 105:403–415.

Reisler, E., C. Smith, and G. Seegan. 1980. Myosin minifilaments. *J. Mol. Biol.* 143:129–145.

Rimm, D. L., D. A. Kaiser, D. Bhandari, P. Maupin, D. P. Kiehart, and T. D. Pollard. 1990. Identification of functional regions on the tail of *Acanthamoeba* myosin-II using recombinant fusion proteins. I. High resolution epitope mapping and characterisation of monoclonal binding sites. *J. Cell Biol.* 111:2405–2416.

Saez, C. G., J. C. Myers, T. B. Shows, and L. A. Leinwand. 1990. Human nonmuscle myosin heavy chain mRNA: generation of diversity through alternative polyadenylation. *Proc. Natl. Acad. Sci. USA.* 87:1164–1168.

Sambrook, J., E. F. Fritsch, and T. Maniatis. 1989. Molecular Cloning: A Laboratory Manual. Second edition. Cold Spring Harbor Laboratory, Cold Spring Harbor, NY.

Sathyamoorthy, V., M. A. L. Atkinson, B. Bowers, and E. D. Korn. 1990. Functional consequences of the proteolytic removal of regulatory serines from the non-helical tailpiece of *Acanthamoeba* myosin II. *Biochemistry.* 29:3793–3797.

Shohet, R. V., M. A. Conti, S. Kawamoto, Y. A. Preston, D. A. Brill, and R. S. Adelstein. 1989. Cloning of the cDNA encoding the myosin heavy chain of a vertebrate cellular myosin. *Proc. Natl. Acad. Sci. USA.* 86: 7726–7730.

Sinard, J. H., and T. D. Pollard. 1989. The effect of heavy chain phosphorylation and solution conditions on the steady state assembly of *Acanthamoeba* myosin II. *J. Cell Biol.* 107:1529–1535.

Sinard, J. H., W. F. Stafford, and T. Pollard. 1989. The mechanism of assembly of *Acanthamoeba* myosin II minifilaments. Minifilaments assemble by three successive dimerisation steps. *J. Cell Biol.* 109:1537–1547.

Sinard, J. H., D. Rimm, and T. Pollard. 1990. Identification of functional regions of the tail of *Acanthamoeba* myosin II using recombinant fusion proteins. II. Association properties of tails with NH2- and COOH- deletions. *J. Cell Biol.* 111:2417–2426.

Squire, J. M. 1981. The Structural Basis of Muscle Contraction. Plenum Publishing Corp., New York. 276 pp.

Strehler, E. E., M-A. Strehler-Page, J-C. Perriard, M. Periasamy, and B. Nadal-Grinard. 1986. Complete nucleotide and encoded amino acid sequence of a mammalian myosin heavy chain gene. Evidence against Intron-dependent Evolution of the rod. *J. Molec. Biol.* 190:291–397.

Suzuki, H., H. Onishi, K. Takahashi, and S. Watanabe. 1978. Structure and function of chicken gizzard myosin. *J. Biochem. (Tokyo).* 84:1529–1542.

Trybus, K. M., T. W. Huiatt, and S. Lowey. 1982. A bent monomeric conformation of myosin from smooth muscle. *Proc. Natl. Acad. Sci. USA.* 79: 6151–6155.

Warwick, H. M., and J. A. Spudich. 1987. Myosin structure and function in cell motility. *Annu. Rev. Cell Biol.* 3:379–421.

Yanagisawa, M., Y. Hamada, Y. Katsuragawa, M. Imamura, T. Mikawa, and T. Masaki. 1987. Complete primary structure of vertebrate smooth muscle myosin heavy chain deduced from its complementary DNA sequence. *J. Mol. Biol.* 198:143–157.